Effect of Al₂(SO₄)₃ Additive on the Properties of Calcined Gypsum Prepared from Flue Gas Desulfurization

Guanji CHENG, Jianying HAO *, Bing GUO, Tao HU, Shengchang WANG

School of Materials Science and Engineering, Taiyuan University of Science and Technology, Taiyuan 030024, China

In order to upgrade the utilization of flue gas desulfurization (FGD) gypsum, crystal modifier aluminum sulfate (Al₂(SO₄)₃) was added into FGD gypsum to prepare calcined gypsum by calcining at normal pressure, and the effect of Al₂(SO₄)₃ addition on the performance of calcined gypsum was studied. The results show that the addition of Al₂(SO₄)₃ to FGD gypsum is slightly beneficial to promote the crystallization of hemihydrate gypsum (HH) along the a-axis direction. The Al₂(SO₄)₃ addition also has a quick-setting effect on gypsum plaster during the hydration process, meanwhile inhibiting the growth of the (020) crystal plane of dihydrate gypsum (DH), then promoting uniform growth and aggregation along the c-axis. The close stacking makes hardened gypsum body dense and improves the strength of calcined gypsum. The strength of calcined gypsum prepared by calcining FGD gypsum with Al₂(SO₄)₃ of 0.6 wt.% at 170 °C for 2 h is the highest. 2 h and 7 d flexural strength are 3.80 MPa and 7.20 MPa, and 2 h and 7 d compressive strength are 9.05 MPa and 19.23 MPa, respectively. In addition, 2 h flexural and compressive strength of the calcined gypsum with 0.6 ~ 1.0 wt.% of Al₂(SO₄)₃ prepared at 170 ~ 180 °C for 2 h increase by 16 ~ 22 % and 20 ~ 33 %, respectively, which is very advantageous for the high value-added reuse of FGD gypsum for the preparation of high-quality calcined gypsum.
Keywords: FGD gypsum, crystal modifier, calcined gypsum, aluminum sulfate, strength.

1. INTRODUCTION

Flue gas desulfurization (FGD) gypsum was widely used in the production of high-strength gypsum (α-HH) , calcined gypsum (β-HH), cement retarder and soil improvement owing to the high content of calcium sulfate dihydrate (DH) and low cost [1 – 4]. Gypsum materials are green building materials with environmental advantages that can replace traditional materials [5]. A decline in the emphasis on environmental programs in the US through the 1980s caused Japan and Germany to take the lead in the FGD, achieving high value-added applications for FGD gypsum early [6]. In 2004, the utilization rate of FGD gypsum produced by the 25 EU member states reached 71 % [7], while it was only 76 % by 2019 in China [8]. The annual production of FGD gypsum in China was relatively enormous, with a total amount exceeding 10^8 tons up to now [9]. Although α-HH had more excellent performance than β-HH, its complicated preparation process led to high cost and low yield. FGD gypsum is easily converted into β-HH at low energy consumption and used to manufacture a large number of gypsum products due to its forming ability and rapid hardening ability [10], and the global gypsum wallboard demand is forecast to grow by 7.2 % annually from 2021 to 2026 [11], which is a feasible and effective green approach.

However, when β-HH came into contact with water, DH crystals usually grew rapidly into needle-like and interlocking structures that were not conducive to the strength of building gypsum. Adding a crystal modifier to regulate the crystallization and control the hydration morphology was the key to create a high value-added and real-scale application of FGD gypsum. Currently, the crystal modifier is mainly used in the preparation of α-HH, including surfactant [12, 13], organic acid (salt) [14 – 16] and inorganic matter [17, 18], while the mechanism of crystal modifier on β-HH was rarely studied. Many highly efficient organic crystal modifiers in α-HH were strong retarders for the hydration of β-HH [19, 20], which was mainly to reduce the supersaturation [19, 21] and delayed the growth habit of DH along the c-axis of gypsum. The morphology ranged from needle-like to short-columnar, which largely weakened the contact areas between the crystals, finally leading to the plummet of the strength of building gypsum. Moreover, inorganic salts had a slight effect on the solubility of gypsum [22], nucleation and hydration kinetics [4, 23] than organic additives, and had certain advantages in the preparation of building gypsum, with excellent stability even at higher temperatures. Numerous studies have been reported that the higher the metal cation valence of inorganic salt, the better its effect on the growth habit of gypsum crystals. Such as Al^{3+}, it had a superior adsorption effect on gypsum and promoted the coarser for α-HH crystals [17, 18].

In this work, Al₂(SO₄)₃ was selected as a crystal modifier to eliminate anion interference. However, the experimental results found that adding more Al₂(SO₄)₃ to FGD gypsum would react with carbonate impurities to generate carbon dioxide gas, which would also destroy the structure of the hardened gypsum during the hydration process. Thus, the effect of adding a small amount of Al₂(SO₄)₃ (≤ 1 wt.%) on the properties of the calcined gypsum was mainly studied, and the transformation mechanism was explored in detail.

---

* Corresponding author. Tel.: +86-18234066956.
E-mail: *jianyinghao@tyust.edu.cn* (J. Hao)

2. EXPERIMENTAL

2.1. Materials

The FGD gypsum came from the Second Thermal Power Plant in Taiyuan and its chemical composition is shown in Table 1. The crystal modifier of $Al_2(SO_4)_3 \cdot 18H_2O$ was pure and purchased from the Tianjin Zhiyuan Chemical Plant.

Table 1. Chemical composition of FGD gypsum (wt.%)

CaO	SO_3	Al_2O_3	MgO	Fe_2O_3	SiO_2	Loss
32.4	42.6	0.8	0.5	0.4	3.4	19.9

2.2. Experimental procedure

A certain amount of $Al_2(SO_4)_3$ was weighed according to 0 wt.%, 0.3 wt.%, 0.6 wt.% and 1.0 wt.% of FGD gypsum and dissolved in the appropriate amount of water. Then the FGD gypsum and the solution were mixed and stirred into a slurry state by a mixer (JJ-5). After the slurry was dried in an oven (101B-2 type) at 40 °C, the dried product was ground into powder and sieved with a standard sieve (aperture: 0.178 mm). To make the powder fully calcined, the thickness of the powder in the square crucible was about 1.2 cm, and the powder was calcined at 140 ~ 180 °C for 2 h and aged for 1 d. The calcined samples were marked as AS-$Al_2(SO_4)_3$ content-calcination temperature, such as AS-0-160 and AS-0.3-160, etc.

2.3. Characterization and test methods

Thermal analysis of FGD gypsum was performed by using TGA/DSC 3+ (Mettler Toledo, Switzerland, 10 °C/min) to estimate dehydration temperature and weight loss with increasing temperature. The phase compositions of calcined gypsum and hydrated gypsum were analyzed by X-ray powder diffraction (XRD, X' Pert PRO type, Cu Kα ray, step length 0.02°). Scanning electron microscopy (SEM S-4800 Philips, Holland) was used to observe the microstructures of calcined gypsum and hydrated gypsum.

According to Chinese standard [24] "Gypsum plaster-determination of physical properties of pure paste", water consumption of standard consistency of gypsum plaster was tested. 300 g sample and mixed water were poured into a mixing pot, and then the mixture was quickly stirred for 30 s and poured into the steel cylinder. The excess slurry was scraped off, so that the slurry surface was flush with the upper end face of the cylinder. The cylinder was lifted at a speed of 150 mm/s when the sample was contacted with water for 50 s. The water of standard consistency was the water/powder ratio when the fluidity of plaster was equal to 180 ± 5 mm. According to the Chinese standard [25] "Calcined gypsum", the properties of calcined gypsum were evaluated, such as setting time, flexural strength and compressive strength. 200 g sample and the water consumption of standard consistency were mixed and quickly stirred for 30 s, subsequently poured into the ring mold with the glass bottom plate and shaken up and down slightly 5 times. Then the mold containing the slurry was put under the needle of the Vicat instrument, and the setting time was counted from the time of adding water. Similarly, a gypsum block (40 mm × 40 mm × 160 mm) was prepared by mixing 300 g of sample and the water consumption of

standard consistency into slurry, pouring into a steel mold to form. The flexural and compressive strength of gypsum block naturally cured for 2 h and 7 d were tested.

According to the hydration and dehydration characteristics of gypsum, the content of the three phases containing anhydrous (AH), hemihydrate (HH) and dihydrate (DH) gypsum was determined. An analytical balance (BSA124S, 0.0001g) was used to weigh 3 g calcined gypsum, named G_1. The weighed sample was put into a weighing bottle. 95 wt.% aqueous ethanol solution was injected to soak the sample completely, and then they were dried in the oven at 40 °C for 2 d with the lid open. Subsequently, the bottle was removed, covered and placed in a dryer to cool to room temperature, and at this time the mass was weighed as G_2. Similar to the above method, a 2 g sample (marked as G_3) was put into a similar bottle and deionized water was also poured to soak the sample completely. After drying at 40 °C for 2 d, the sample was put to the dryer to cool to room temperature, and its mass was marked as G_4. Finally, 1 g sample (marked as G_5) was weighed and placed in the oven at 300 °C for 2 h, and cooled to room temperature in the dryer. Its mass was recorded as G_6. The three-phase gypsum calculation Eq. 1 – Eq. 3 [26] were as follows:

$$AH\% = 1511 \times (b - 1); \tag{1}$$

$$HH\% = 537 \times (c + 3 - 4b); \tag{2}$$

$$DH\% = 159 \times (4b - c - 3x); \tag{3}$$

($b=G_1/G_2$, $c=G_3/G_4$, $x=G_6/G_5$, when $b < 1$, $AH = 0$).

The heat release of gypsum plaster during the hydration process was measured by Probe Thermometer (TP 101). Simultaneously, the 100 g sample and the water consumption of standard consistency were quickly stirred for 30 s, then the plaster was poured into the thermos cup and sealed. Finally, the probe thermometer was inserted into the plaster from the upper cup hole, and the temperature of the hydration per minute was recorded.

3. RESULTS AND DISCUSSION

### 3.1. Thermal analysis of FGD gypsum

The thermogravimetric curve and micromorphology of FGD gypsum are shown in Fig. 1 a and b, respectively. In Fig. 1 a, there is an endothermic peak in the range of 105 ~ 180 °C, attributing to the removal of crystal water, and the corresponding weight loss is about 19.8 %. The morphology of FGD gypsum is irregular lamellar crystals surrounded by fine amorphous particles in Fig. 1 b, and the average particle size is about 45 μm.

3.2. XRD analysis of calcined gypsum

The XRD patterns of the calcined gypsum with and without $Al_2(SO_4)_3$ at different temperatures are detected in Fig. 2. As can be seen from Fig. 2 a, without the addition of $Al_2(SO_4)_3$, the diffraction peak intensity of HH (PDF#41-0224) is gradually mounting with the increase of temperature, while that of DH (PDF#21-0816) gradually decreases and then disappears at 180 °C. The XRD patterns of the calcined gypsum with 0.6 wt.% $Al_2(SO_4)_3$ at different temperatures are displayed in Fig. 2 b. The peak intensity of

the crystal plane (400) of HH calcined at 170 ~ 180 °C is higher than that of other temperatures, indicating that the dehydration of DH into HH is facilitated by raising temperature. The XRD patterns of the calcined gypsum containing different amounts of $Al_2(SO_4)_3$ at 170 °C are presented in Fig. 2 c. The (200) and (400) planes peak intensity of HH is slightly improved as containing 0.6 ~ 1.0 wt.% $Al_2(SO_4)_3$, suggesting that the $Al_2(SO_4)_3$ addition can promote the growth of HH crystals in the a-axis direction, which is beneficial to improve the quality of calcined gypsum.

Guo [27] found that when the calcination temperature was between 160 and 220 °C, HH partially continued to dehydrate and transformed into anhydrites (AH). Therefore, the diffraction peaks of AH (PDF#43-0606) are reflected in Fig. 2. However, the diffraction peaks of HH and AH are too close together to distinguish them by comparing (PDF#41-0224) with (PDF#43-0606) [28], and may also exist together. Therefore, the three-phase test method is chosen.
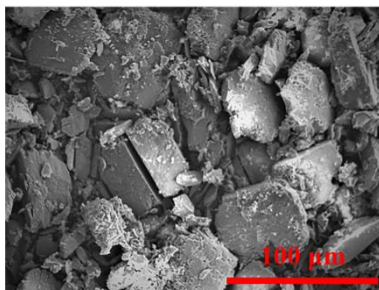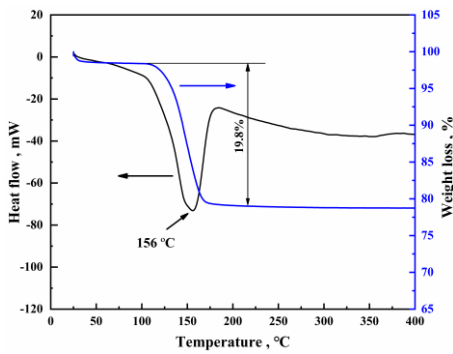
Fig. 1. a – TG and DSC curves; b – SEM image of FGD

Naturally, the three-phase test theory of gypsum is an efficient method to determine the three phases (DH, HH, AH) content of calcined gypsum and the results are shown in Table 2. The calcination temperature is more sensitive to the content of different phases. The content of DH is higher at 160 °C, while it is the least at 180 °C, which is consistent with the above results. Besides, the content of HH increases and then decreases, while the content of AH gradually increases with the increase in temperature. AH has a stronger water absorption capacity and larger expansion rate than HH, thus AH causes more water consumption and crystal internal stress to destroy the strength of hardened gypsum. In addition, a large amount of AH needs to absorb moisture in the air and is transformed into HH by aging. Nevertheless, it is advisable to control the residual DH since it has no bonding ability and is the most harmful to the
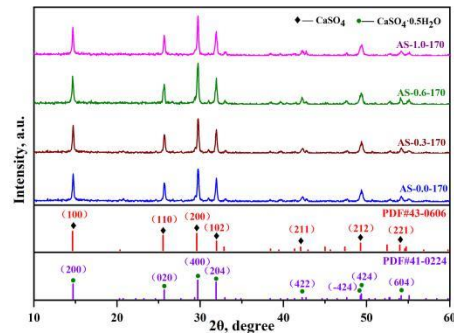
performance of hardened gypsum. According to the content of HH, it is inferred that the appropriate calcination temperature is 170 °C.
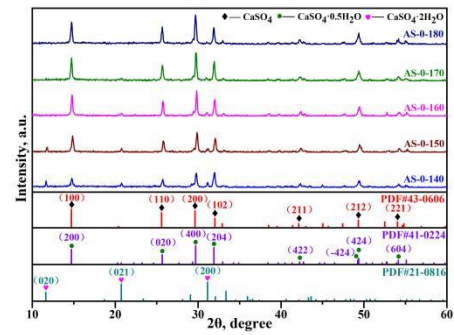
a
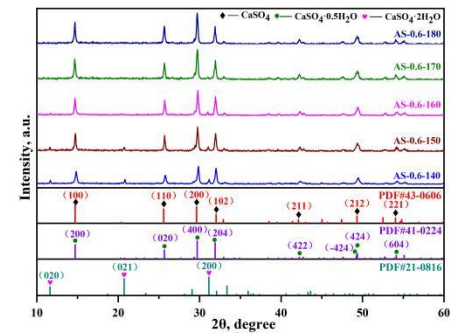
b

c

Fig. 2. XRD patterns of the calcined gypsum: a – without $Al_2(SO_4)_3$; b – with 0.6 wt% of $Al_2(SO_4)_3$ at different temperatures; c – containing different contents of $Al_2(SO_4)_3$ at 170 °C

Table 2. Three phases content of calcined gypsum (wt.%)

Sample	DH	HH	AH
AS-0-160	14.35	82.89	2.76
AS-0-170	3.93	84.53	11.54
AS-0-180	3.54	74.71	21.75
AS-0.3-160	14.25	83.59	2.16
AS-0.3-170	3.45	84.83	11.72
AS-0.3-180	3.03	75.27	21.7
AS-0.6-160	13.47	82.71	3.82
AS-0.6-170	3.09	85.68	11.23
AS-0.6-180	2.17	75.52	22.31
AS-1.0-160	13.85	82.51	3.64
AS-1.0-170	3.28	85.97	10.75
AS-1.0-180	2.83	75.06	22.11

3.3. Performance of building plaster

The water consumption of standard consistency and setting time of calcined gypsum with $Al_2(SO_4)_3$ are plotted in Fig. 3 a and b, respectively. The water consumption, and initial and final setting time of building plaster gradually increase with rising calcination temperature in Fig. 3 a and b. This is because the calcined gypsum prepared at 160 °C has much residual DH, and the higher the calcination temperature, the greater the total content of HH and AH in the calcined gypsum. The hydration rates of HH and AH are usually fast, and AH has the highest hydration activity and reacts with more water, thereby its hydration process is much longer than that of HH. This is the reason why the water consumption and setting time are greatly increased as calcined at 180 °C compared with 170 °C.

a

b
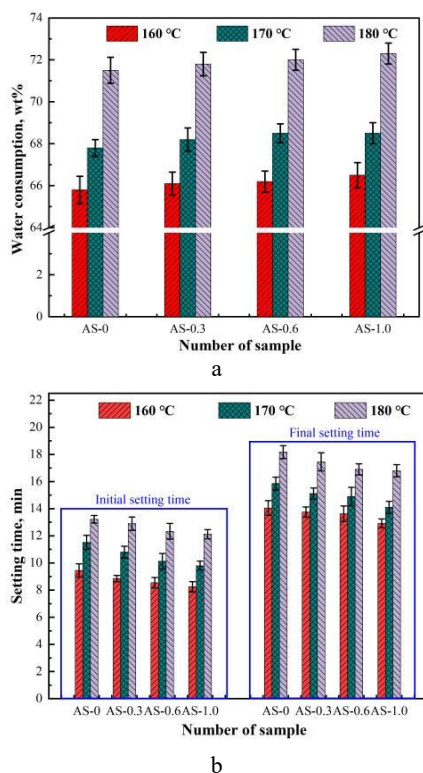
Fig. 3. a – water consumption of standard consistency; b – setting time of gypsum plaster

With the increase of $Al_2(SO_4)_3$ addition, the water consumption of plaster slightly increases, while the initial and final setting time is slightly shortened. $Al_2(SO_4)_3$ has an early setting effect on the hydration of building plaster, mainly because the introduction of SO_4^{2-} can improve the supersaturation of DH to promote its hydration, thereby accelerating the formation of the initial crystalline network structure [29]. Thus, more water is needed to achieve standard consistency for the calcined gypsum. Generally, more water consumption may prolong the settling time of gypsum plaster. However, combined with the quick setting effect of $Al_2(SO_4)_3$, the resultant setting time is shortened due to the increase in $Al_2(SO_4)_3$ content. Rashad [30] also found that the addition of Al^{3+} decreased the induction time of gypsum crystals formation. The initial setting time of calcined gypsum is concentrated between 8 ~ 13.5 min, and the final setting time focuses on 13 ~ 19 min, which conforms to the standard requirements. The standard stipulates that the initial setting time shall not be less than 3 min and the final setting time shall not be more than 30 min [25]. Overall, the faster setting rates can result in higher gypsum strength [31].

3.4. Hydration heat

The hydration heat of gypsum plaster can be calculated by Eq. 4 where Q represents heat, c is specific heat capacity, m is mass, t_1 is initial temperature and t_2 is final temperature. The change of plaster temperature with time is shown in Fig. 4. It is proportional to the heat of hydration since c and m are constant here. The hydration temperature of gypsum plaster with 0.6 wt.% of $Al_2(SO_4)_3$ prepared at different temperatures is displayed in Fig. 4 a. Obviously, the higher the calcination temperature, the more the exothermic heat of the gypsum plaster, and the faster the hydration exothermic rate within 0 ~ 3 min. However, the second exothermic heat process exhibits an opposite trend. This is because the calcined gypsum prepared at lower temperature contains less AH and more DH acts as hydrated nuclei to quickly promote the hydration of HH. On the contrary, the calcined gypsum prepared at a higher temperature has more HH and AH that will release more hydration heat. Generally, AH can prolong the hydration reaction more than HH, which is consistent with the above results of setting time and Guo's discovery [27].

$$Q = cm(t_2 - t_1). \qquad (4)$$

a

b
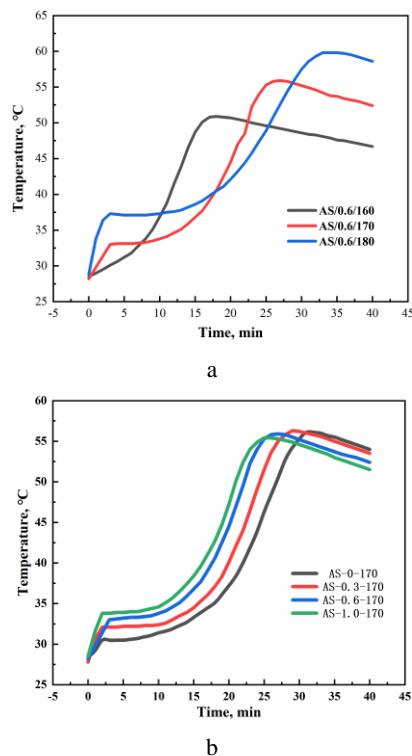
Fig. 4. The hydration temperature of gypsum plaster: a – with 0.6 wt.% of $Al_2(SO_4)_3$ at different temperatures; b – containing different amounts of $Al_2(SO_4)_3$ at 170 °C

The effect of $Al_2(SO_4)_3$ content on the hydration heat of gypsum plaster is shown in Fig. 4 b. It can be seen that the hydration reaction is accelerated with the mounting content of $Al_2(SO_4)_3$, but the total exothermic heat is nearly equal. Therefore, the exothermic heat rate can also indicate that

$Al_2(SO_4)_3$ has a rapid setting effect on gypsum plaster, mainly because the SO_4^{2-} in $Al_2(SO_4)_3$ can improve the supersaturation of DH and facilitate its nucleation and growth. In addition, it can be found that the gypsum plaster can quickly release much heat within minutes of the final setting by combining the setting time with the hydration time, as shown by the second peak in Fig. 4 b.

3.5. Strength of calcined gypsum

The flexural and compressive strength of the calcined gypsum containing $Al_2(SO_4)_3$ cured for 2 h and 7 d are shown in Fig. 5 a and b, respectively. The mechanical strength of hardened gypsum first increases and then decreases with elevating calcination temperature, and the strength reaches its highest when calcined at 170 °C.

a

b
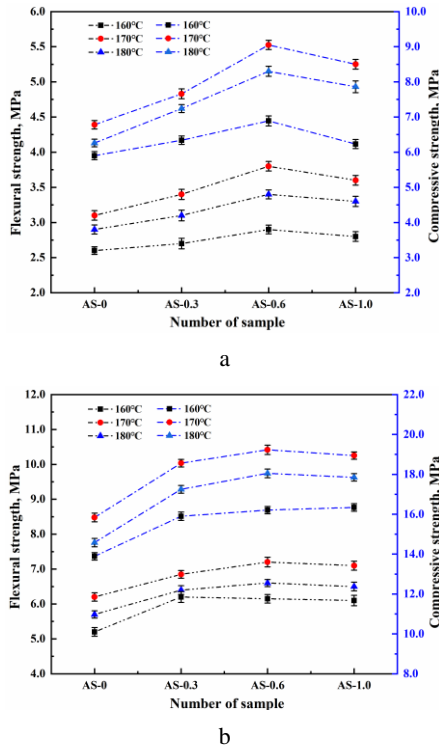
Fig. 5. Flexural and compressive strength of calcined gypsum in different curing periods: a – 2 h; b – 7 d

Because the dehydration of calcined gypsum is insufficient at 160 °C and the results in Table 2 also show that the residual DH content is relatively higher than that of other temperatures. As calcined at 170 °C, the content of HH is highest, while the content of DH is reduced dramatically. HH has excellent bonding ability, followed by AH. When the calcined temperature is up to 180 °C, the strength of hardened gypsum decreases, while it is higher than that of 160 °C. The main reason is that the content of AH at 180 °C exceeds 20 wt.%, leading to the increase of water consumption during the hydration process. More water consumption will isolate the crystals and reduce the contact area between the crystals. Thus, it is difficult to obtain a dense hardened body if the setting rate is too slow. In addition, AH will induce micro expansion after the hydration, which can result in stress inside the crystal structure. Subsequently, the resultant micro-cracks are easy to expand forward, reducing the strength of gypsum. Moreover, the strength of gypsum is higher than that of

gypsum calcined at 160 °C. This is because AH can be transformed into HH by aging and is less harmful to calcined gypsum than DH.

In Fig. 5, the strength of calcined gypsum containing $Al_2(SO_4)_3$ is higher than that without $Al_2(SO_4)_3$, and the flexural and compressive strength first increase and then decreases with the increase of $Al_2(SO_4)_3$ content. 2 h flexural and compressive strength is enhanced by 16 ~ 22 % and 20 ~ 33 %, respectively. Besides, the strength of calcined gypsum with 0.6 wt.% of $Al_2(SO_4)_3$ is maximum especially when prepared at 170 °C. 2 h flexural and compressive strength are 3.80 MPa and 9.05 MPa, and 7 d flexural and compressive strength are up to 7.2 MPa and 19.23 MPa, respectively, which is much higher than the previous results reported by the research group [3]. This may be because Al^{3+} change the crystal habit of DH, which makes the DH of a hardened body grow and overlap densely. However, the strength of hardened gypsum with 1.0 wt.% of $Al_2(SO_4)_3$ slightly decreases, mainly because more Al^{3+} will react with carbonate impurities in calcined gypsum to generate CO_2, leading to destroy the internal structure of hydrated gypsum. According to Chinese standard [25], the calcined gypsum containing 0.3 ~ 1.0 wt.% $Al_2(SO_4)_3$ prepared at 170 °C meets grade 3.0. Grade 3.0 calcined gypsum requires 2 h flexural and compressive strength are ≥ 3 MPa and ≥ 6 MPa, respectively.

3.6. XRD analysis of hardened gypsum

The XRD patterns of hardened gypsum are presented in Fig. 6. It is found that the main phase of hardened gypsum cured for 7 d is DH. The diffraction peak intensity of the (020) crystal plane of DH decreases with the increase of $Al_2(SO_4)_3$ content, indicating that Al^{3+} inhibits the growth of the crystal plane and promotes the growth of DH along the c-axis. According to the orientation analysis of the calcium sulfate molecular layer during the transformation of DH gypsum, the molecular layer of the (010) plane in the DH crystal is transformed into the (001) plane of HH gypsum during the dehydration process.
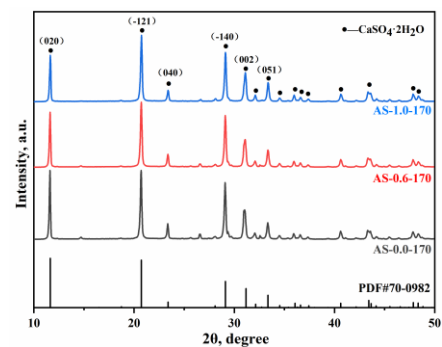
Fig. 6. XRD patterns of the hardened gypsum cured for 7 d

Fan [17] also confirmed the preferential adsorption of Al^{3+} on the surface of HH crystals by XPS and ICP-OES, and observed that Al^{3+} significantly inhibited the growth of HH along the c-axis. The position of Al^{3+} in the crystal structure was shown to be preferentially adsorbed on the active sites of the (002) plane by molecular dynamics simulations, which suppressed the growth rate and resulted in the formation of short rod-like HH. In turn, Al^{3+} can

inhibit the growth of the (020) crystal plane of DH in the hydration process.

3.7. Morphology analysis of hardened gypsum

SEM images of hardened gypsum cured for 2 h and 7 d are displayed in Fig. 7. In Fig. 7 a, the residual HH crystals are wrapped in the newly formed crystals, indicating that the hydration time of 2 h is short and the reaction is insufficient. With the extension of the curing period, the remaining HH crystals continue to be dissolved by the surrounding residual water. And DH crystals formed will precipitate and grow on the initial crystal network structure, leading to densification until the solution is supersaturated, as shown in Fig. 7 a and b. This is why the mechanical strength of calcined gypsum can be largely improved after the hydration of 7 d. The similar results are obtained by comparing Fig. 7 e with Fig. 7 f. As HH comes in contact with water, water will quickly enter the cracks and pores of HH to dissolve, resulting in quick supersaturation and crystallization. The network skeleton structure of DH is rapidly formed in a very short time, which seriously inhibits the flow of the plaster and slows down the hydration rate.

DH crystals without $Al_2(SO_4)_3$ can freely grow into interlocking and needle-like structures in Fig. 7 b, causing less contact area between the crystals and low strength. After 0.6 wt.% of $Al_2(SO_4)_3$ is added, DH crystals are evenly distributed and tend to the same growth direction since the Al^{3+} has strong adsorption capacity [17] on the surface of gypsum crystals and make the gypsum crystals aggregate [30] to reduce the surface energy. That can affect the growth habit of (020) crystal plane, resulting in more aggregate and denser between the crystals in Fig. 7 f. In addition, grain boundaries can be observed after the hydration of HH, indicating water molecules contacted with HH will quickly enter the dehydrated pore and more defective slits [28] to dissolve. To illustrate better the phenomenon, a low magnification of 1000 times is chosen to observe the micromorphology of the overall hydrated body after the hydration of 7 d, such as Fig. 7 c and g. The morphology with the addition of $Al_2(SO_4)_3$ is denser than that without $Al_2(SO_4)_3$. As is shown in Fig. 7 d and h,

magnified by 5000 times, it can be seen that the former are loose and interlocked needle-like structures with more pores, while the grains of the latter are uniformly distributed and clustered on the whole.

The DH crystal belongs to the monoclinic system, and its growth rates of planes are very different due to the different bonding formation and binding energies of SO_4^{2-} and Ca^{2+} in different axis directions. If the growth rate of the (010) plane is 1.00, the growth rate of the (110) plane is 1.76 and that of the (111) plane is 1.88 [32]. In the absence of additives, the ideal crystals are unmodified and bilaterally symmetrical flat hexagonal prism [33], which is consistent with the crystals circled in red in Fig. 7 d. However, the presence of Al^{3+} will inhibit the growth of the (020) plane and facilitate the growth of DH crystal along the c-axis.

3.8. Analysis of transformation mechanism

The micromorphology of the calcined gypsum containing 0.6 wt.% $Al_2(SO_4)_3$ prepared at 160 ~ 180 °C is presented in Fig. 8. The calcined gypsum at 160 °C in Fig. 8 a shows countless small one-way pores due to the removal of partial water. The water molecules in the gypsum are removed from the surface layer to the inside. Further mounting calcination temperature, as shown in Fig. 8 b and c, the structure of gypsum particles is becoming more and more loose, especially in Fig. 8 c. The dissociation starts from the top angle of gypsum particles. At this time, micro-cracks appear and expand, and then the gypsum crystals split. Due to the nearly 30 % difference in molar volume between DH (74.23 cm³/mol) and HH (53.21 cm³/mol), expansion and contraction occur during the thermal decomposition of DH into HH, which leads to crack development and delamination. Finally, countless small amorphous particles are easily dehydrated into AH. This is similar to Pedreno-Rojas's discovery that the gypsum particles gradually degraded with mounting calcination temperature [34]. Therefore, the higher the calcination temperature, the greater the water consumption during the hydration and hardening of calcined gypsum, which is in general agreement with the results in Fig. 3.
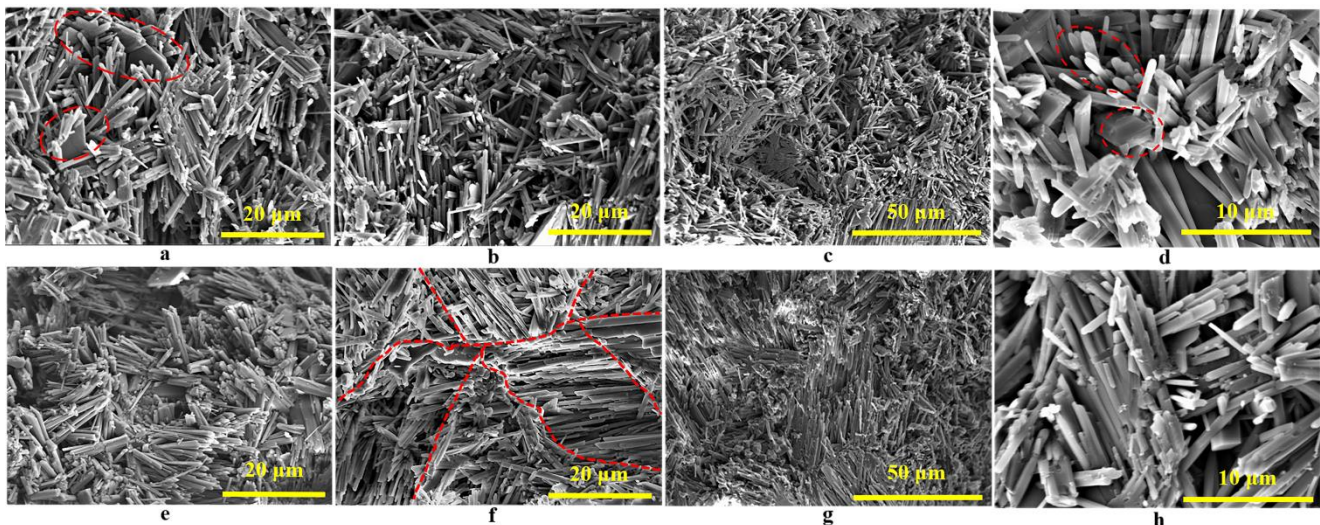

Fig. 7. SEM images of the hydrated product of hardened gypsum: a – AS-0-170-2h; b, c, d – AS-0-170-7d; e – AS-0.6-170-2h; f, g, h – AS-0.6-170-7d
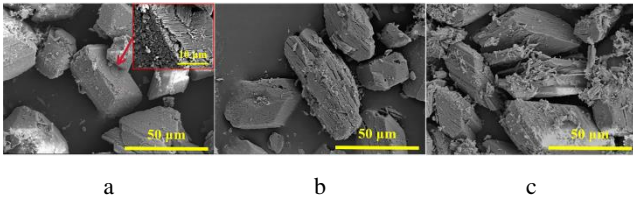
Fig. 8. SEM images of the calcined gypsum adding 0.6 wt.% $Al_2(SO_4)_3$ at different temperatures: a – 160 °C; b – 170 °C; c – 180 °C

In short, the gypsum particles are cleaved by layers and split from angles during the calcination of FGD gypsum.

The hydration mechanism of building plaster is shown in Fig. 9. The particles of obliquely prismatic β-HH are rapidly dissolved upon contact with the aqueous solution, and water molecules enter the interior of its particles through microcracks and slit holes and dissolve in reverse. The surface of particles then becomes smooth. The solution quickly reaches the supersaturation and DH crystals gradually precipitate. As the hydration time increases, the particles continue to dissolve and split where microcracks exist inside. The precipitated DH crystals grow and interlock with each other, resulting in the gradual increase in the interlocking degree of the network skeleton structure of the gypsum hardened body and the rapid increase in the strength.
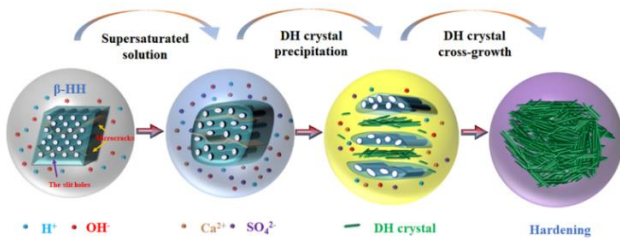
Fig. 9. The hydration mechanism of building plaster

4. CONCLUSIONS

The crystal modifier of $Al_2(SO_4)_3$ is added to FGD gypsum to produce calcined gypsum by calcining at 140 ~ 180 °C for 2 h. The diffraction peak intensity of the (400) crystal plane of HH is slightly enhanced by adding 0.6 ~ 1.0 wt.% $Al_2(SO_4)_3$, which promotes the growth of HH crystals in the a-axis direction.

On the contrary, the new growth of the (020) crystal plane of DH is inhibited during the hydration process since the Al^{3+} has strong adsorption capacity on the crystal surface of DH to decrease surface energy and SO_4^{2-} has a fast setting effect on gypsum plaster, which promotes its uniform growth and aggregation along the c-axis. Therefore, $Al_2(SO_4)_3$ addition can make the hardened gypsum body denser, improving the strength of calcined gypsum.

The calcined gypsum prepared by FGD gypsum with 0.6 wt.% $Al_2(SO_4)_3$ calcined at 170 °C has the highest strength. 2 h and 7 d flexural strength are 3.8 MPa and 7.2 MPa, and 2 h and 7 d compressive strength are 9.05 MPa and 19.23 MPa, respectively. In addition, FGD gypsum containing 0.6 ~ 1.0 wt.% $Al_2(SO_4)_3$ is calcined at 170 ~ 180 °C for 2 h, 2 h flexural and compressive strength are increased by 16 ~ 22 % and 20 ~ 33 %, respectively,

compared with that of FGD gypsum without $Al_2(SO_4)_3$, which is beneficial to the large-scale resource utilization of FGD gypsum.

REFERENCES

1. **Truman, C.C., Nuti, R.C., Truman, L.R., Dean, J.D.** Feasibility of Using FGD Gypsum to Conserve Water and Reduce Erosion from an Agricultural Soil in Georgia *Catena* 81 (3) 2010: pp. 234 – 239.
https://dio.org/10.1016/j.catena.2010.04.003

2. **Jiang, G.M., Wang, H., Chen, Q.S., Zhang, X.M., Wu, Z.B., Guan, B.H.** Preparation of alpha-Calcium Sulfate Hemihydrate from FGD Gypsum in Chloride-Free $Ca(NO_3)_2$ Solution under Mild Conditions *Fuel* 174 2016: pp. 235 – 241.
https://dio.org/10.1016/j.fuel.2016.01.073

3. **Hao, J., Cheng, G., Hu, T., Guo, B., Li, X.** Preparation of High-Performance Building Gypsum by Calcining FGD Gypsum Adding CaO as Crystal Modifier *Construction and Building Materials* 306 2021: pp. 124910.
https://doi.org/10.1016/j.conbuildmat.2021.124910

4. **Song, K.M., Mitchell, J., Jaffel, H., Gladden, L.F.** Simultaneous Monitoring of Hydration Kinetics, Microstructural Evolution, and Surface Interactions in Hydrating Gypsum Plaster in the Presence of Additives *Journal of Materials Science* 45 (19) 2010: pp. 5282 – 5290.
https://dio.org/10.1007/s10853-010-4572-7

5. **Benjeddou, O., Soussi, C., Benali, M., Alyousef, R.** Experimental Investigation of a New Ecological Block Made by Mixing Gypsum Plaster and Desert Sand *Arabian Journal for Science and Engineering* 45 (5) 2020: pp. 4037 – 4052.
https://doi.org/10.1007/s13369-020-04362-4

6. **Bruce, B.** Global Gypsum Megatrends-Does the Past Predict the Future; accessed 03 January 2011.
https://www.globalgypsum.com/magazine/articles/325-global-gypsum-megatrends-does-the-past-predict-the-future

7. **Leiva, C., García Arenas, C., Vilches, L.F., Vale, J., Gimenez, A., Ballesteros, J.C., Fernández-Pereira, C.** Use of FGD Gypsum in Fire Resistant Panels *Waste Management* 30 (6) 2010: pp. 1123 – 1129.
https://doi.org/10.1016/j.wasman.2010.01.028

8. **Liu, F.** How Far Is the Road to Break; accessed 09 November 2020. https://m.thepaper.cn/baijiahao_9911992

9. **Liu, S., Liu, W., Jiao, F., Qin, W., Yang, C.** Production and Resource Utilization of Flue Gas Desulfurized Gypsum in China – A Review *Environmental Pollution* 288 2021: pp. 117799.
https://doi.org/10.1016/j.envpol.2021.117799

10. **Del Río-Merino, M., Vidales-Barriguete, A., Piña-Ramírez, C., Vitiello, V., Santa Cruz-Astorqui, J., Castelluccio, R.** A Review of the Research about Gypsum Mortars with Waste Aggregates *Journal of Building Engineering* 45 2022: pp. 103338.
https://doi.org/10.1016/j.jobe.2021.103338

11. **Staff.** Global Gypsum Wallboard Demand Forecast to Grow by 7.2% Annually between 2021 and 2026; accessed 21 April

2022. https://www.globalgypsum.com/news/item/1821-global-gypsum-wallboard-demand-forecast-to-grow-by-7-2-annually-between-2021-and-2026

12. **Zhang, X.F., Wang, J.S., Wu, J.S., Jia, X.J., Du, Y.C., Li, H.Y., Zhao, B.X.** Phase- and Morphology-Controlled Crystallization of Gypsum by Using Flue-Gas-Desulfurization Gypsum Solid Waste *Journal of Alloys and Compounds* 674 2016: pp. 200–206. https://dio.org/10.1016/j.jallcom.2016.03.021

13. **Mao, X.L., Song, X.F., Lu, G.M., Xu, Y.X., Sun, Y.Z., Yu, J.G.** Effect of Additives on the Morphology of Calcium Sulfate Hemihydrate: Experimental and Molecular Dynamics Simulation Studies *Chemical Engineering Journal* 278 2015: pp. 320–327. https://dio.org/10.1016/j.cej.2014.10.006

14. **Jia, C.Y., Chen, Q.S., Zhou, X., Wang, H., Jiang, G.M., Guan, B.H.** Trace NaCl and Na$_2$EDTA Mediated Synthesis of alpha-Calcium Sulfate Hemihydrate in Glycerol-Water Solution *Industrial & Engineering Chemistry Research* 55 (34) 2016: pp. 9189–9194. https://org/10.1021/acs.iecr.6b02064

15. **Lanzón, M., García-Ruiz, P.A.** Effect of Citric Acid on Setting Inhibition and Mechanical Properties of Gypsum Building Plasters *Construction and Building Materials* 28 (1) 2012: pp. 506–511. https://doi.org/10.1016/j.conbuildmat.2011.06.072

16. **Nilles, V., Plank, J.** Study of the Retarding Mechanism of Linear Sodium Polyphosphates on α-Calcium Sulfate Hemihydrate *Cement and Concrete Research* 42 (5) 2012: pp. 736–744. https://doi.org/10.1016/j.cemconres.2012.02.008

17. **Fan, H., Song, X.F., Liu, T.J., Xu, Y.X., Yu, J.G.** Effect of Al^{3+} on Crystal Morphology and Size of Calcium Sulfate Hemihydrate: Experimental and Molecular Dynamics Simulation Study *Journal of Crystal Growth* 495 2018: pp. 29–36. https://dio.org/10.1016/j.jcrysgro.2018.05.013

18. **Zhao, W.P., Gao, C.H., Zhang, G.Y., Xu, J., Wang, C.X., Wu, Y.M.** Controlling the Morphology of Calcium Sulfate Hemihydrate Using Aluminum Chloride as a Habit Modifier *New Journal of Chemistry* 40 (4) 2016: pp. 3104–3108. https://dio.org/10.1039/c5nj02804c

19. **Ziegenheim, S., Sztegura, A., Szabados, M., Kónya, Z., Kukovecz, Á., Pálinkó, I., Sipos, P.** EDTA Analogues – Unconventional Inhibitors of Gypsum Precipitation *Journal of Molecular Structure* 1256 2022: pp. 132491. https://dio.org/10.1016/j.molstruc.2022.132491

20. **Mao, X.L., Song, X.F., Lu, G.M., Sun, Y.Z., Xu, Y.X., Yu, J.G.** Control of Crystal Morphology and Size of Calcium Sulfate Whiskers in Aqueous HCl Solutions by Additives: Experimental and Molecular Dynamics Simulation Studies *Industrial & Engineering Chemistry Research* 54 (17) 2015: pp. 4781–4787. https://dio.org/10.1021/acs.iecr.5b00585

21. **Liu, S.T., Nancollas, G.H.** A Kinetic and Morphological Study of the Seeded Growth of Calcium Sulfate Dihydrate in the Presence of Additives *Journal of Colloid & Interface Science* 52 (3) 1975: pp. 593–601. https://dio.org/10.1016/0021-9797(75)90285-4

22. **Li, Z., Demopoulos, G.P.** Effect of NaCl, MgCl$_2$, FeCl$_2$, FeCl$_3$, and AlCl$_3$ on Solubility of CaSO$_4$ Phases in Aqueous HCl or HCl + CaCl$_2$ Solutions at 298 to 353 K *Journal of Chemical & Engineering Data* 51 (51) 2006: pp. 569–576. https://dio.org/10.1021/je0504055

23. **Rabizadeh, T., Stawski, T.M., Morgan, D.J., Peacock, C.L., Benning, L.G.** The Effects of Inorganic Additives on the Nucleation and Growth Kinetics of Calcium Sulfate Dihydrate Crystals *Crystal Growth & Design* 17 (2) 2017: pp. 582–589. https://dio.org/10.1021/acs.cgd.6b01441

24. **GB/T17669.4-1999.** Chinese National Standards: Gypsum Plasters-Determination of Physical Properties of Pure Paste. 1999.

25. **GB/T9776-2008**. Chinese National Standards: Calcined Gypsum. 2008.

26. **Chen, Y., Yue, W., Dong, R.** Gypsum Building Material *China Building Materials Industry Press*, Beijing, 2012.

27. **Guo, H.S., Wang, Q.P., Li, W.F., Feng, X., Yang, J.L., Cao, J.J., Shen, T.Z., Qin, X.M., Liu, Y.F., Gui, Y.H., Zhou, L.M.** Phase Transformation and Physical Properties of Binding Materials Fabricated from Solid Waste FGD Gypsum by Oil Bath Heating and the Micromorphology and Formation Mechanism of Their Hydration Products *Construction and Building Materials* 377 2023: pp. 130981. https://doi.org/10.1016/j.conbuildmat.2023.130981

28. **Chen, X., Wu, Q., Gao, J., Tang, Y.** Hydration Characteristics and Mechanism Analysis of β-Calcium Sulfate Hemihydrate *Construction and Building Materials* 296 2021: pp. 123714. https://dio.org/10.1016/j.conbuildmat.2021.123714

29. **Ahmadi Moghadam, H., Mirzaei, A.** Comparing the Effects of a Retarder and Accelerator on Properties of Gypsum Building Plaster *Journal of Building Engineering* 28 2020: pp. 101075. https://doi.org/10.1016/j.jobe.2019.101075

30. **Rashad, M.M., Mahmoud, M.H.H., Ibrahim, I.A., Abdel-Aal, E.A.** Crystallization of Calcium Sulfate Dihydrate under Simulated Conditions of Phosphoric Acid Production in the Presence of Aluminum and Magnesium Ions *Journal of Crystal Growth* 267 (1) 2004: pp. 372–379. https://doi.org/10.1016/j.jcrysgro.2004.03.060

31. **Ye, Q., Guan, B., Lou, W., Yang, L., Kong, B.** Effect of Particle Size Distribution on the Hydration and Compressive Strength Development of α-Calcium Sulfate Hemihydrate Paste *Powder Technology* 207 (1) 2011: pp. 208–214. https://doi.org/10.1016/j.powtec.2010.11.001

32. **Follner, S., Wolter, A., Helming, K., Silber, C., Bartels, H., Follner, H.** On the Real Structure of Gypsum Crystals *Crystal Research and Technology* 37 (2–3) 2002: pp. 207–218. https://doi.org/10.1002/1521-4079(200202)37:2/33.0.CO;2-L

33. **Cody, A.M., Cody, R.D.** Chiral Habit Modifications of Gypsum from Epitaxial-like Adsorption of Stereospecific Growth Inhibitors *Journal of Crystal Growth* 113 1991: pp. 508–519. https://dio.org/10.1016/0022-0248(91)90086-K

34. **Pedreño-Rojas, M.A., De Brito, J., Flores-Colen, I., Pereira, M.F.C., Rubio-de-Hita, P.** Influence of Gypsum Wastes on the Workability of Plasters: Heating Process and Microstructural Analysis *Journal of Building Engineering* 29 2020: pp. 101143. https://doi.org/10.1016/j.jobe.2019.101143